Hybrid kinetic model of the magnetosheath plasma cloud penetration through the magnetopause and comparison with MMS observations. Preliminary results

Alexander S. Lipatov[a,c], Levon A. Avanov[b,c], Barbara L. Giles[c], Daniel J. Gershman[c]

[a] UMBC, Baltimore, MD 21250

[b] UMCP, College Park, MD 20742

[c] NASA GSFC, Greenbelt, MD 20771

Fall AGU 2023 Meeting, San Francisco, CA, December 11 - 15, 2023

1. Questions to be answered with hybrid modeling:

The aim of our research is a study of the effects of the plasma clouds (plasmoids) penetration across the magnetopause. MMS provides an opportunity to study plasma cloud transport with high resolution plasma and field data. By modeling this event accurately, we can validate our model and help to understand plasma cloud transport in general, which has relevance to a lot of astrophysical systems.

In this Report the magnetopause is considered as a **tangential discontinuity** with the parallel magnetic field in the magnetosheath and magnetosphere.

The plasma parameters (**magnetosheath bulk velocity, particle temperatures, plasma density and magnetic field; plasma cloud velocity, thermal velocity, size and density**) were chosen from the MMS observations (case of March 7, 2016) and other observed cases.

Basic science questions:

- (1) **Plasma cloud deformation** and **a strong phase mixing** with magnetospheric plasma;
- (2) **The transfer of energy, mass, and momentum** of the magnetosheath and cloud plasma into magnetospheric plasma;
- (3) **Necessary conditions** for the plasma cloud penetration through the magnetopause;
- (4) **Wave generation by the plasma clouds** inside the magnetopause.

2. Ion acceleration by the plasma cloud observed by MMS spacecraft (A) which was predicted in the hybrid kinetic modeling by Lipatov, Avanov, Giles [JGR 2022] (B)

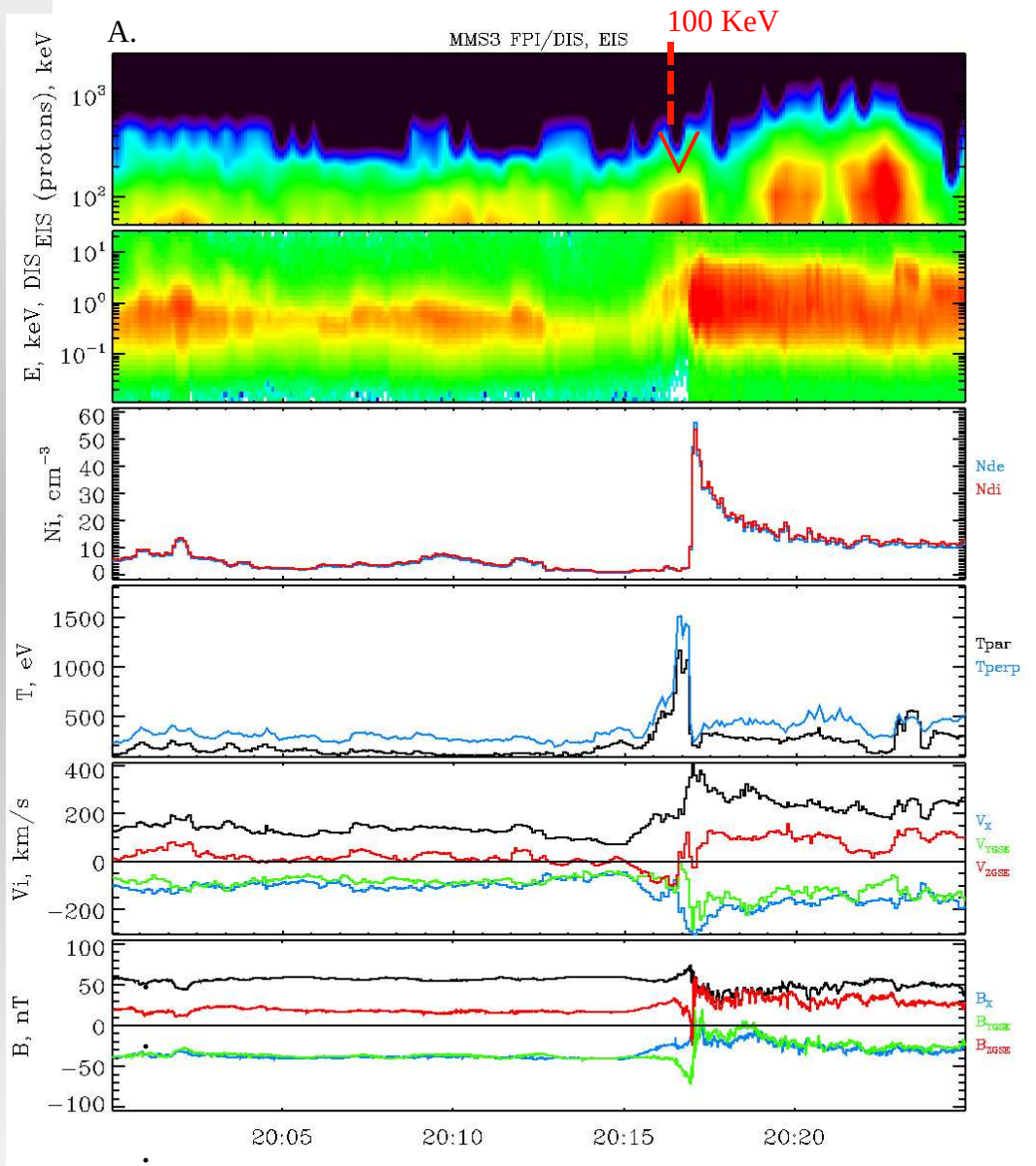

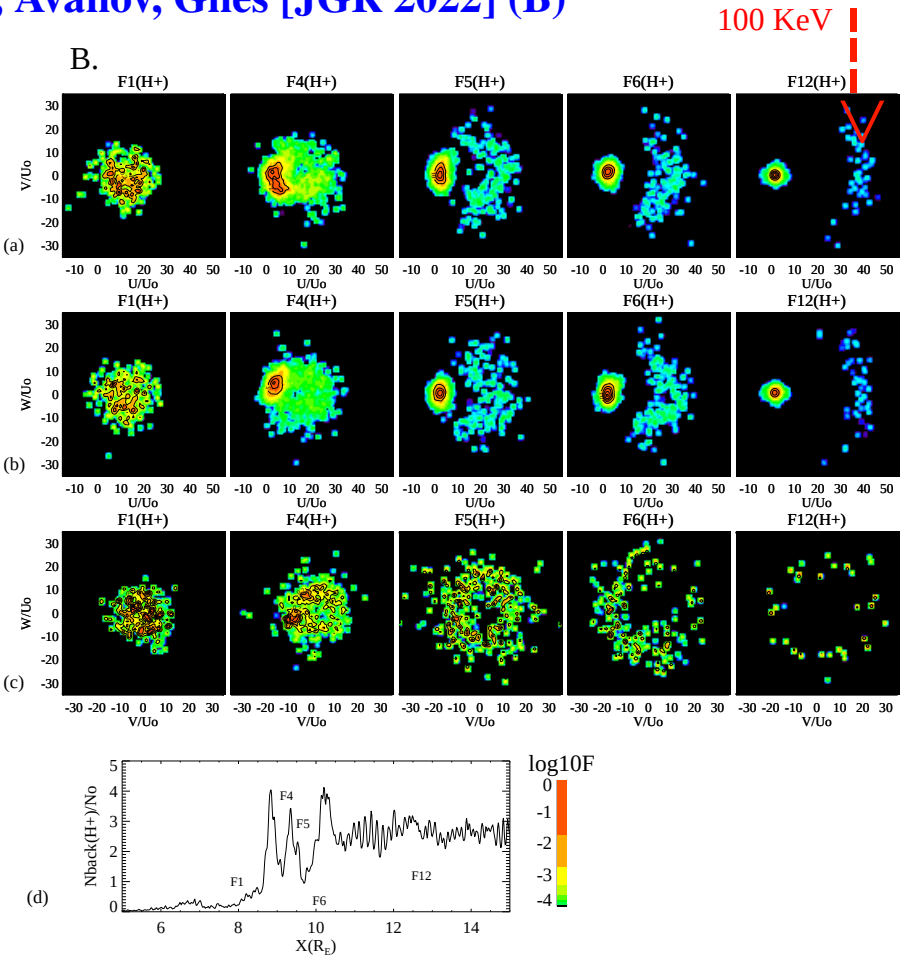

WILEY: Your research makes a difference
1,287,734 – Full text views

for Lipatov, Avanov, & Giles, JGR 2022

MMS observations provide a good validation our numerical model

3. Multi-Target Electromagnetic Shape Function Kinetic (EM-SFK) Method.

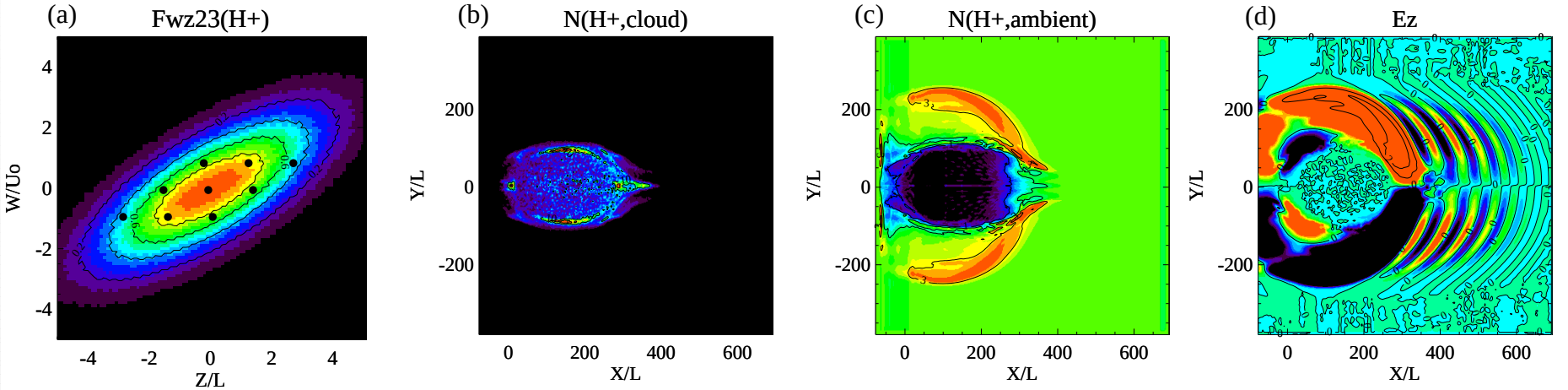

Left: SFK element with point particles. Right: Example of an interaction between the Plasma Cloud and ambient magnetospheric plasma from the modeling with a new 3-D hybrid kinetic EM-SFK method. The higher quality of the numerical solution was produced with only one macro-particle (**location of the particle's center of mass plus deformation matrix**) per cell distribution. The 3-D spatial grid had 257x257x257 cells and 3^6**-point quadrature rule** were used for time evolution of the Gaussian macro-particles in the 6-dimension phase space. Updated virtual point particles were used to construct the **updated covariance matrices**. **This modeling requires only 10GB RAM on laptop/Aitken, whereas it needs 500GB RAM with the Standard PIC method).** Need a re-mapping: Richarson–Lucy algorithm, Direct splitting of the macro-particle over the neighboring cells. References: Larson & Young (JCP, 2015), Bishop (Springer, 2006), Gauger et al. (SIAM, 2000), Alard & Colombi (MNRAS, 2005), Lipatov et al.(ESSOAR, 2022).

4. 2.5-D hybrid simulation of the cloud penetration across tangential discontinuity (TD)

1) Wave generation by a finite size supersonic plasma cloud under penetration through the TD.
2-D contour plots of (left) the ion density and (right) the distribution of total current in the $x - z$ plane at $t = 0.10T_{ci}$. From Lipatov, Sharma and Papadopoulos (1994) and Lipatov (1996, 2002).
2) Deep cloud penetration and a formation of twin vortices in magnetosphere in 2-D Hall-MHD (Huba, 1996) and 2.5-D hybrid (Savoini, Scholer, Fujimoto, 1994) large time modeling. Note that the law of cloud expansion is different in 2-D and 3-D modeling.

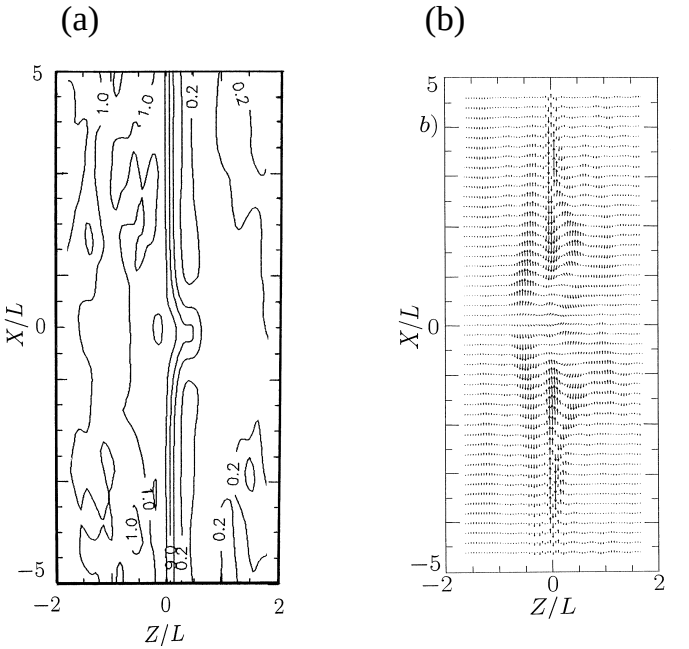

5. MMS satellite observations of the plasma cloud at time 2016-03-07, 00:00:00–01:40:00 UTC

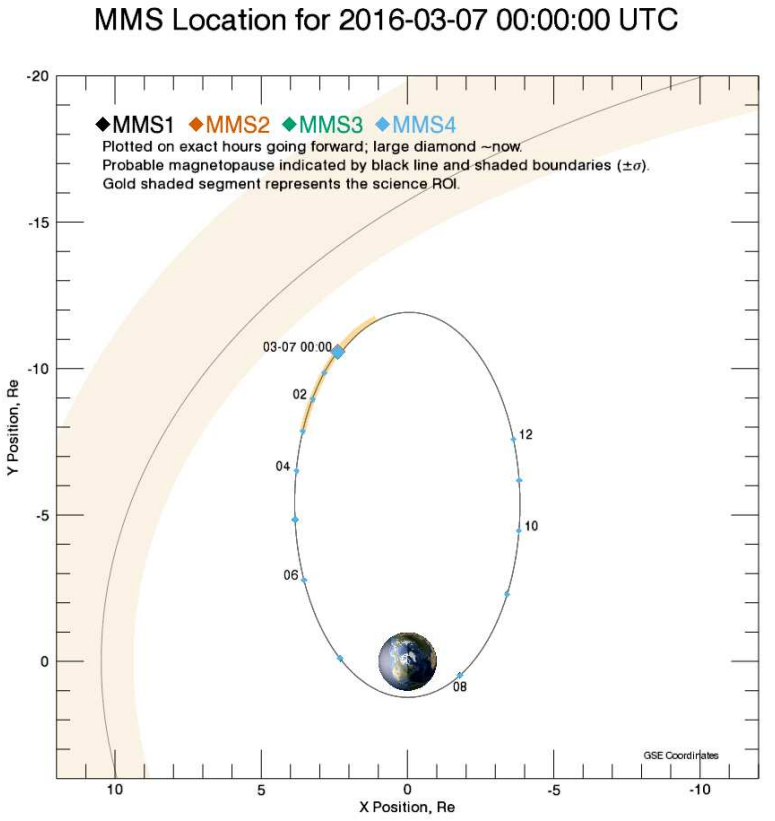

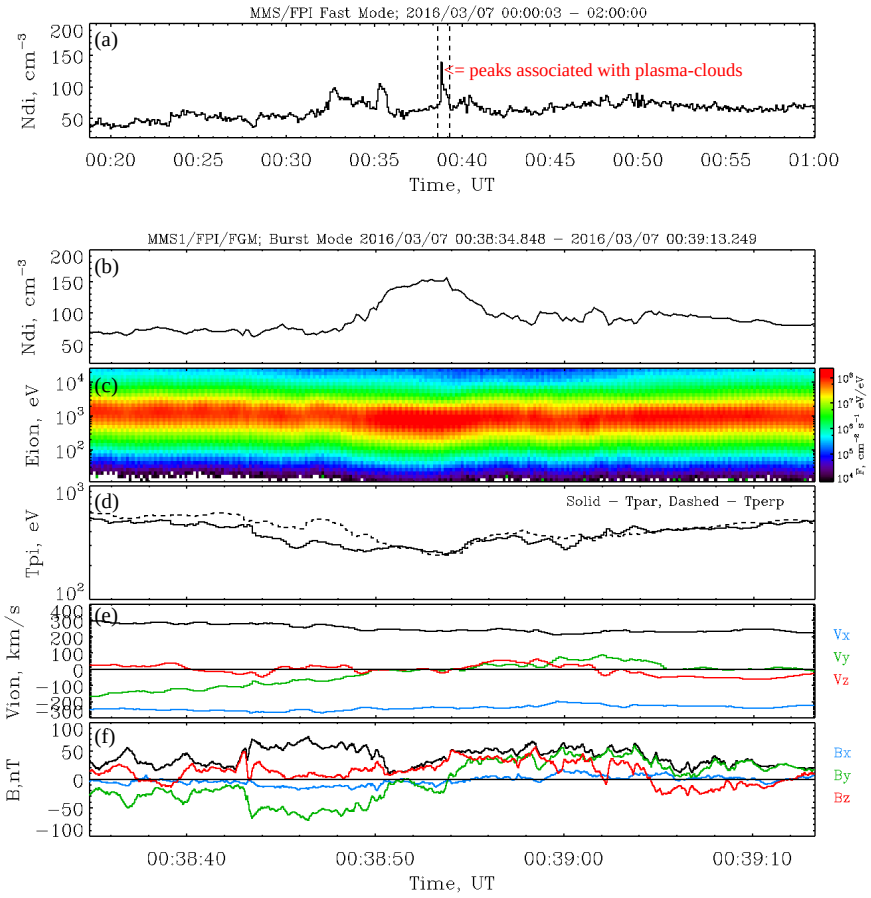

Data are based on the Fast Plasma Investigation (FPI) (Pollock et al., 2016) and

two MMS flux-gate magnetometers (Russell et al., 2016).

5-A. Data analysis of the MMS satellite observations of the plasma cloud at time

2016-03-07, 00:00:00–01:40:00 UTC

Our recent MMS data analysis shows:

Fast mode. The density peaks are in the range from $N_{PC} \approx 100\,\mathrm{cm}^{-3}$ to $N_{PC} \approx 150\,\mathrm{cm}^{-3}$ (a).

Burst mode. The peaks of density vary from $70\,\mathrm{cm}^{-3}$ to $150\,\mathrm{cm}^{-3}$ (b).

The energy of the cloud ions is slightly lower than the energy of the magnetosheath ions (c).

Ion temperature is lower inside cloud (d).

Cloud speed: $V_x \approx -240\,\mathrm{km/sec}$, $V_y \approx 0\,\mathrm{km/sec}$ and $V_z \approx 0\,\mathrm{km/sec}$ (e).

Excitation of the transverse waves upstream the plasma cloud (f).

Size of cloud: $D_x \approx 2400\,\mathrm{km}$, $D_y \approx 1000\,\mathrm{km}$ and $D_z \approx 200\,\mathrm{km}$.

Need the Machine-Learning to split magnetosheath and plasma cloud energy spectra.

6. Set up magnetosheath, magnetospheric plasma and cloud configuration in our modeling.

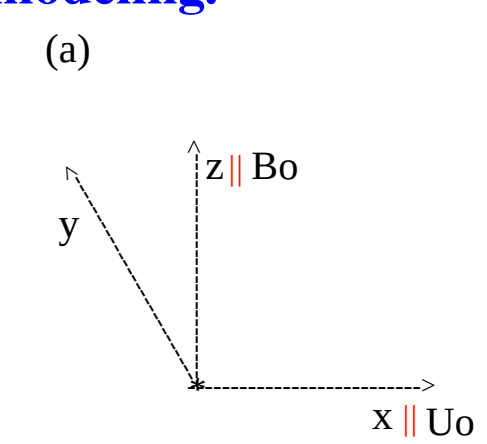

Modeling system of coordinates

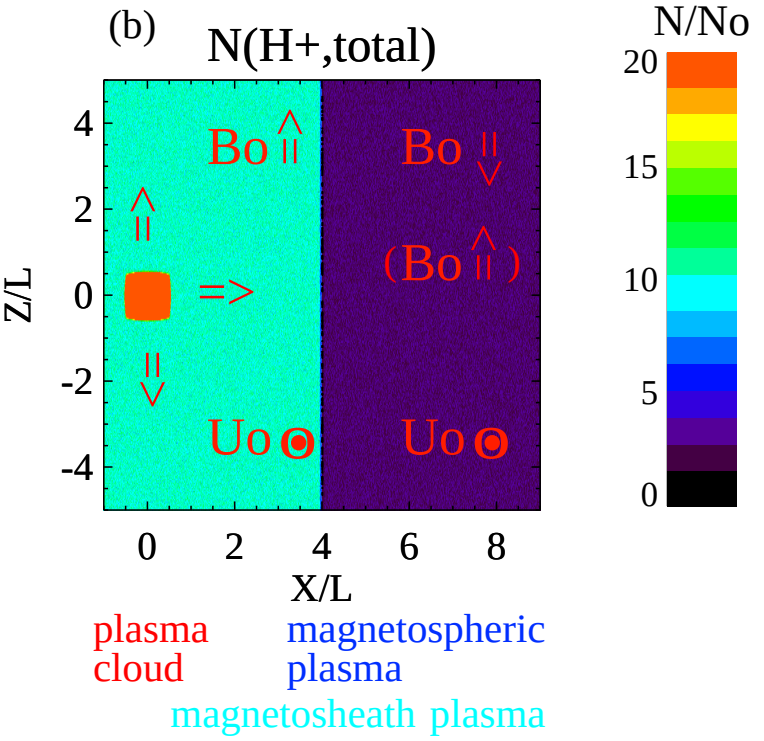

Magnetosheath initial parameters: density: $N_i = 10 - 60\,\mathrm{cm}^{-3}$; thermal velocities: $V_{th,i} = 60 - 140\,\mathrm{km/s}$; $V_{th,e} = 1000\,\mathrm{km/s}$; bulk velocity: $U = 0$: Alfvenic velocity: $V_A \approx (80 - 200)\,\mathrm{km/s}$; and $B = (0; 30; 0)\,\mathrm{nT}$.

Magnetosphere initial parameters: density: $N_i = 2.4\,\mathrm{cm}^{-3}$; thermal velocities: $V_{th,i} \approx 100\,\mathrm{km/s}$; $V_{th,e} \approx 2500\,\mathrm{km/s}$; bulk velocity: $U = 0$: Alfvenic velocity: $V_A = 780\,\mathrm{km/s}$; and $B = (0; 60; 0)\,\mathrm{nT}$.

Plasma cloud initial parameters: Gaussian 3-D profile for density: $\sigma \approx 440\,\mathrm{km}$; $N_i = (60 - 110)\,\mathrm{cm}^{-3}$; $U = (-350[-700]; 0; 0)\,\mathrm{km/s}$; $V_{th,i} \approx 1 - 50\,\mathrm{km/s}$; $V_{th,e} \approx 2500\,\mathrm{km/s}$.

7–A. Dense magnetosheath and fast initial plasma cloud speed

RUN – 88ghkhha; $L = 200$ km;
Cloud speed $Ux = 700$ km/s;
Initial plasma density and
ion thermal velocity:
(a) Plasma cloud: $N_{i,cloud} \approx 110\,\mathrm{cm}^{-3}$;
$V_{th,i} \approx 10$ km/s;
(b) Magnetosheath: $\approx 60\,\mathrm{cm}^{-3}$;
$V_{th,i} \approx 60$ km/s;
(c) Magnetosphere: $\approx 2.4\,\mathrm{cm}^{-3}$;
$V_{th,i} \approx 100$ km/s.
Top: Cloud density;
Middle: Magnetospheric density;
Bottom: Magnetosheath density.

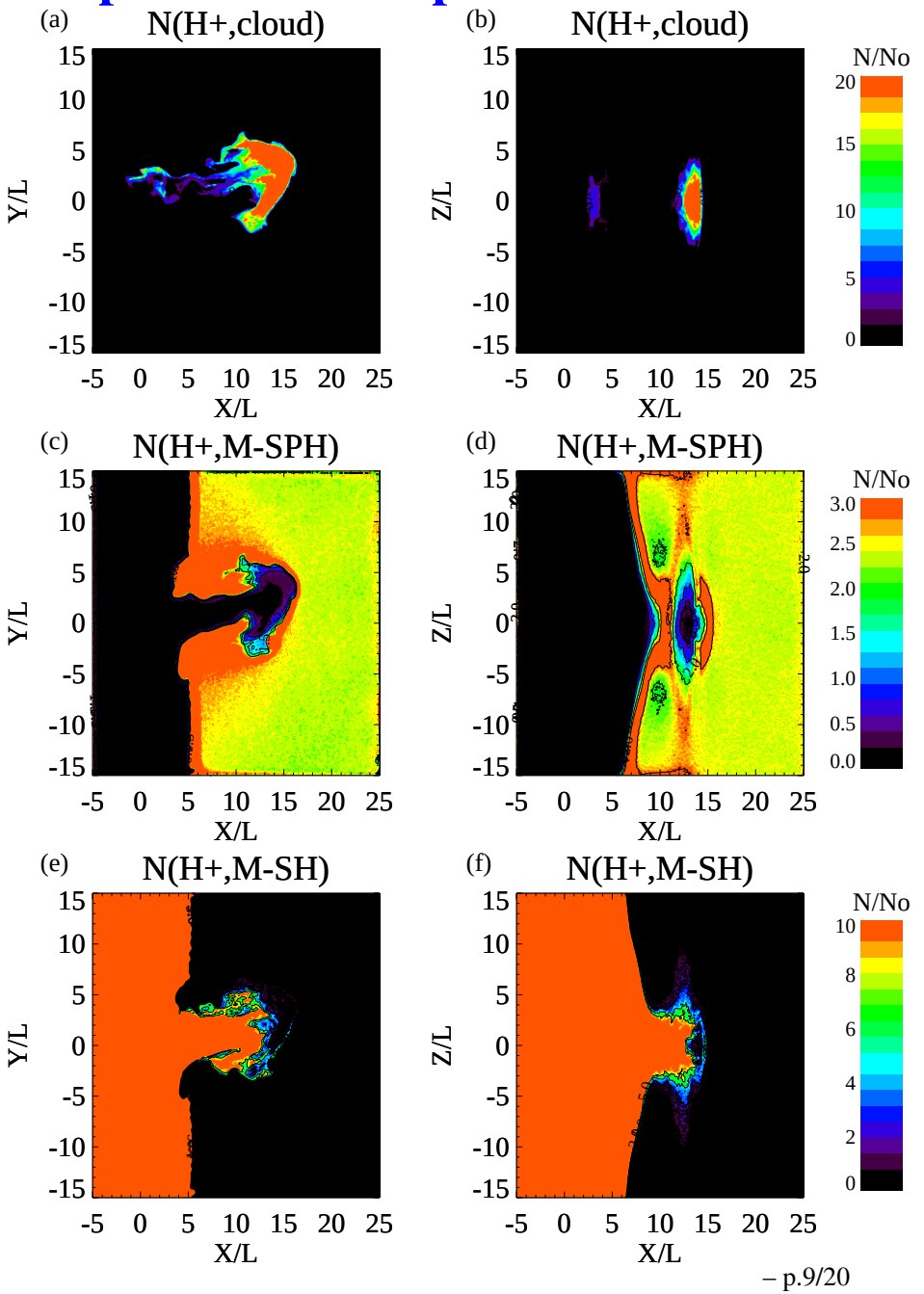

7–B. Magnetic Field and Kinetic Energy Distribution

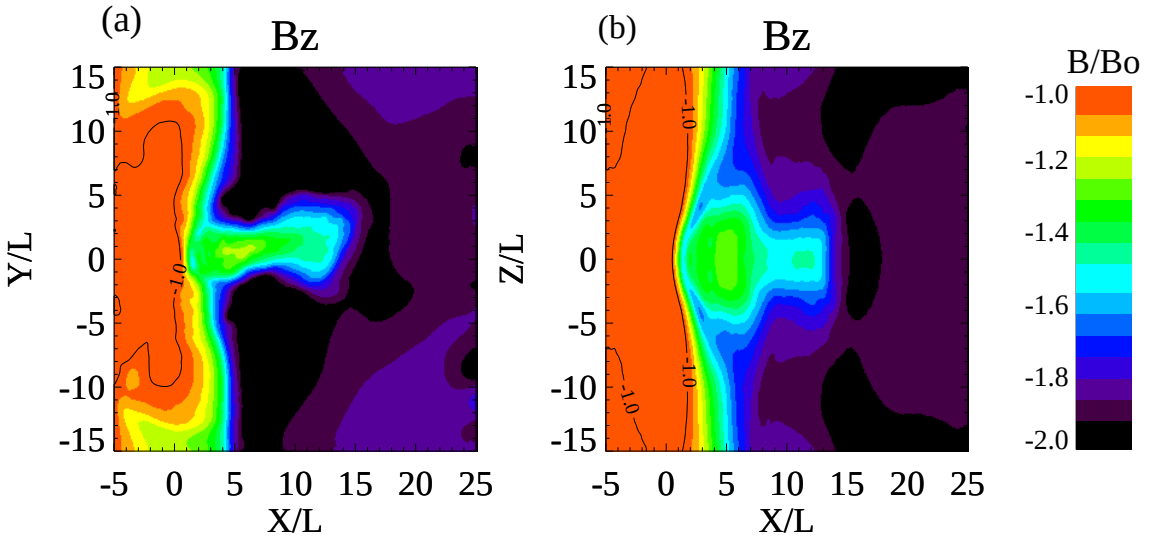

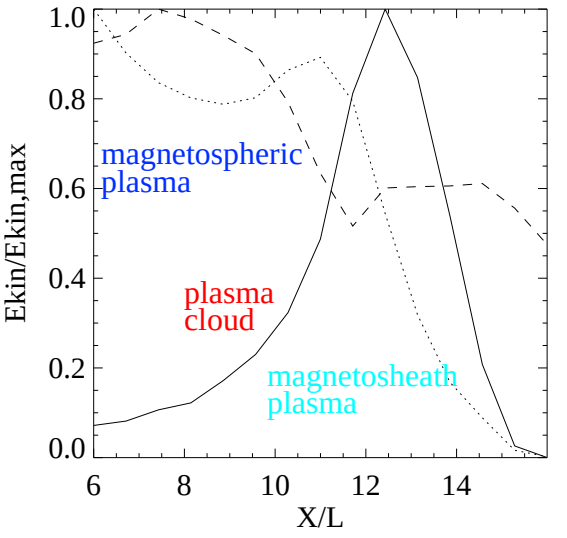

7–C. VDF of Plasma Cloud Ions

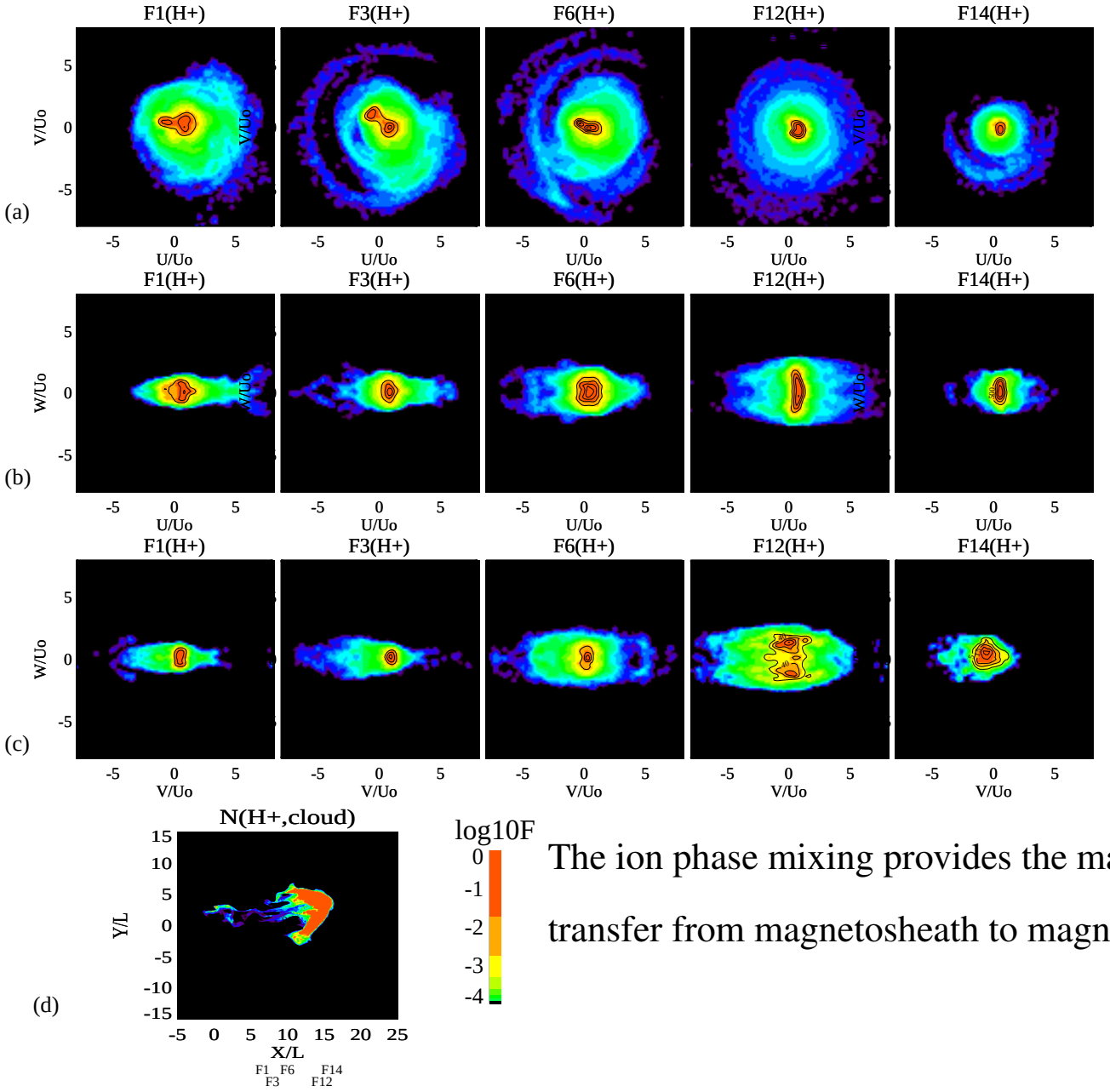

The ion phase mixing provides the mass, momentum and energy transfer from magnetosheath to magnetosphere.

7–D. VDF of Magnetospheric Ions

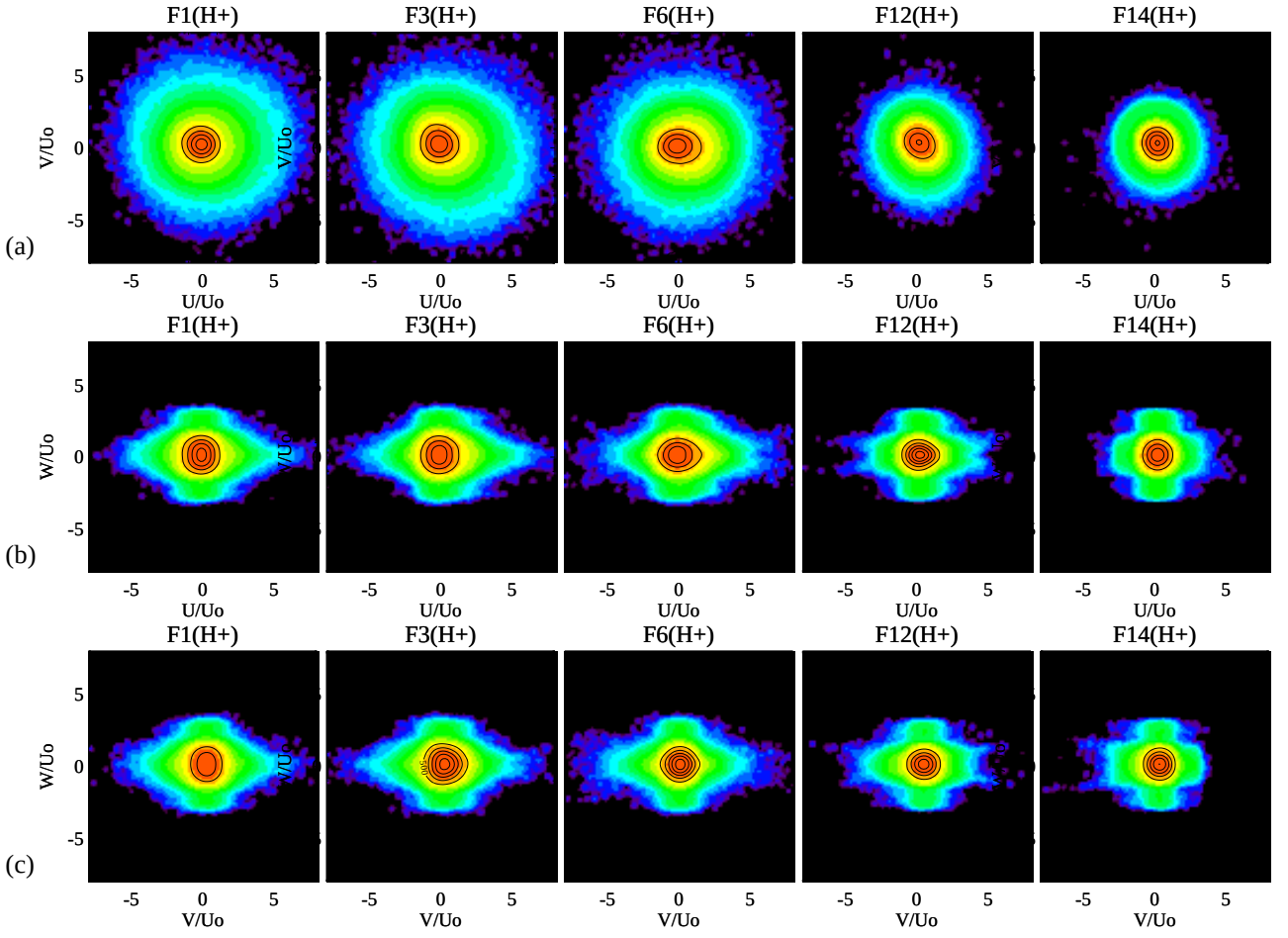

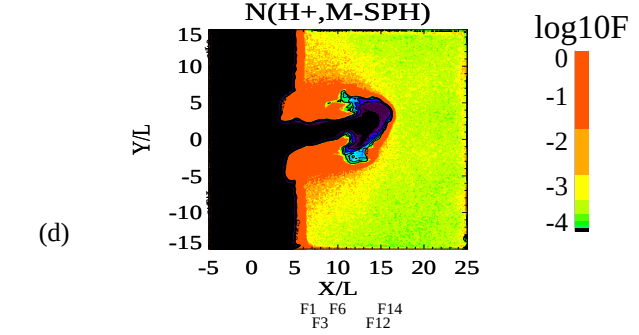

The ion phase mixing provides the mass, momentum and energy transfer from magnetosheath to magnetosphere.

7–E. VDF of Magnetosheath Ions

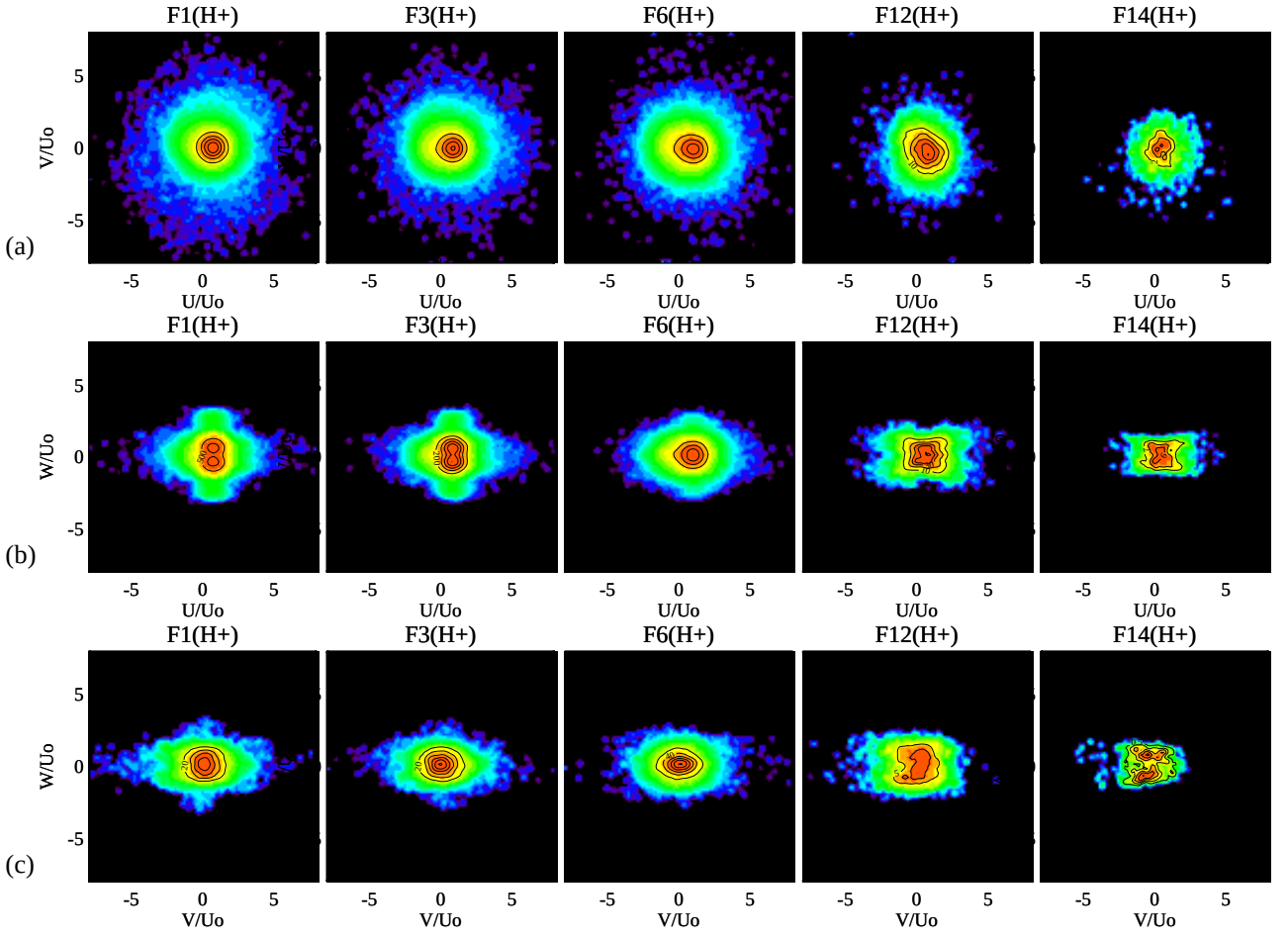

The ion phase mixing provides the mass, momentum and energy transfer from magnetosheath to magnetosphere.

8. Plasma cloud penetration via magnetopause in case of low magnetosheath density and fast initial speed

RUN – 48ghc; $L = 400\,\text{km}$;
Cloud speed $Ux = 700\,\text{km/s}$;
Initial plasma density and
ion thermal velocity:
(a) Plasma cloud: $N_{i,cloud} \approx 110\,\text{cm}^{-3}$;
$V_{th,i} \approx 10\,\text{km/s}$;
(b) Magnetosheath: $N_i \approx 10\,\text{cm}^{-3}$;
$V_{th,i} \approx 100\,\text{km/s}$;
(c) Magnetosphere: $N_i \approx 2.4\,\text{cm}^{-3}$.
$V_{th,i} \approx 100\,\text{km/s}$.
Top: Cloud density;
Middle: Magnetospheric density;
Bottom: Magnetosheath density.

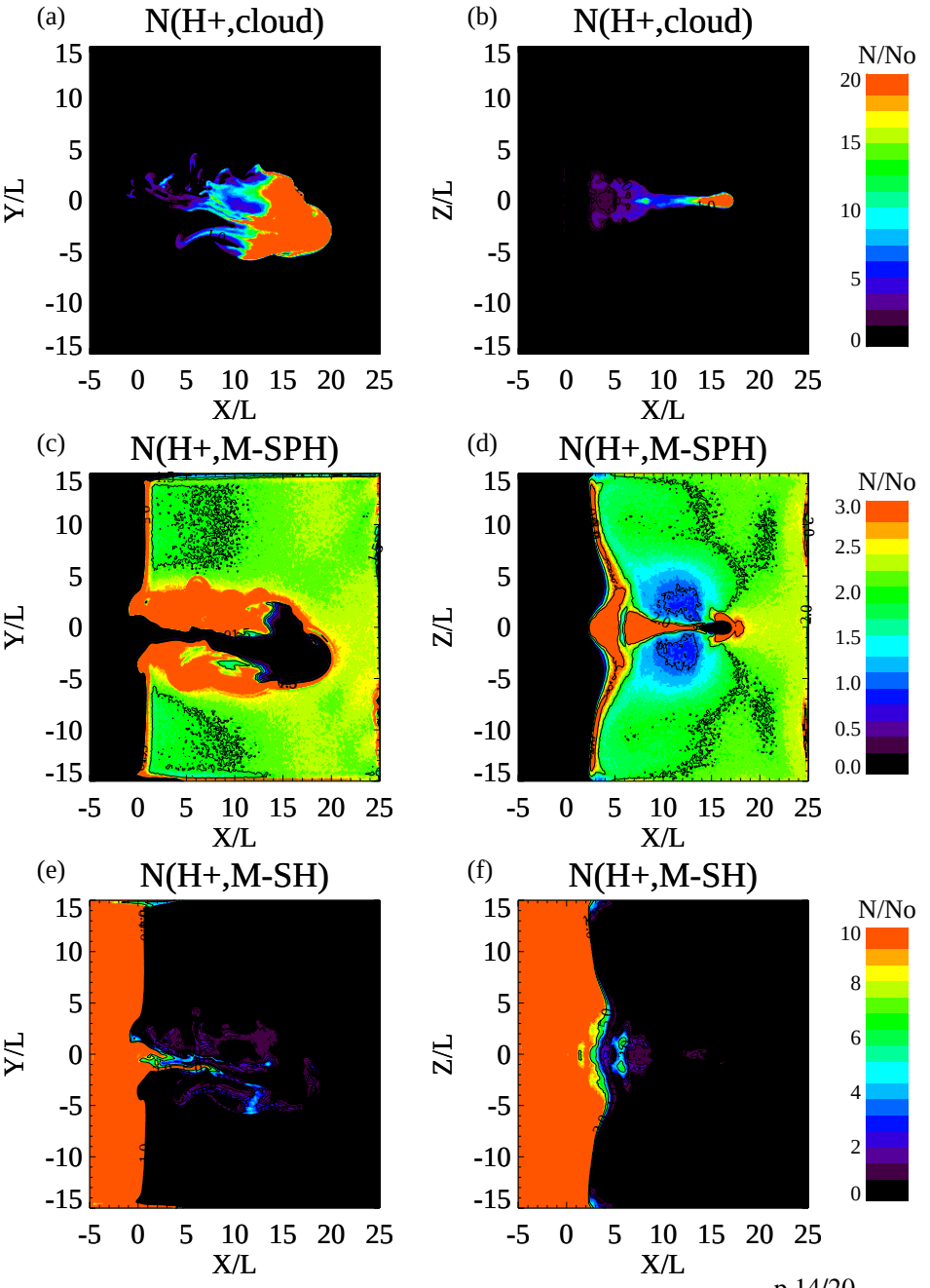

9. Dense magnetosheath, moderate initial plasma cloud speed but short initial distance to magnetopause

RUN – 88ghkhhb; $L = 200\,\mathrm{km}$;
Cloud speed $Ux = 300\,\mathrm{km/s}$;
Initial plasma density and
ion thermal velocity:
(a) Plasma cloud: $N_{i,cloud} \approx 110\,\mathrm{cm}^{-3}$;
$V_{th,i} \approx 10\,\mathrm{km/s}$;
(b) Magnetosheath: $\approx 60\,\mathrm{cm}^{-3}$;
$V_{th,i} \approx 60\,\mathrm{km/s}$;
(c) Magnetosphere: $\approx 2.5\,\mathrm{cm}^{-3}$;
$V_{th,i} \approx 100\,\mathrm{km/s}$.
Top: Cloud density;
Middle: Magnetospheric density;
Bottom: Magnetosheath density.

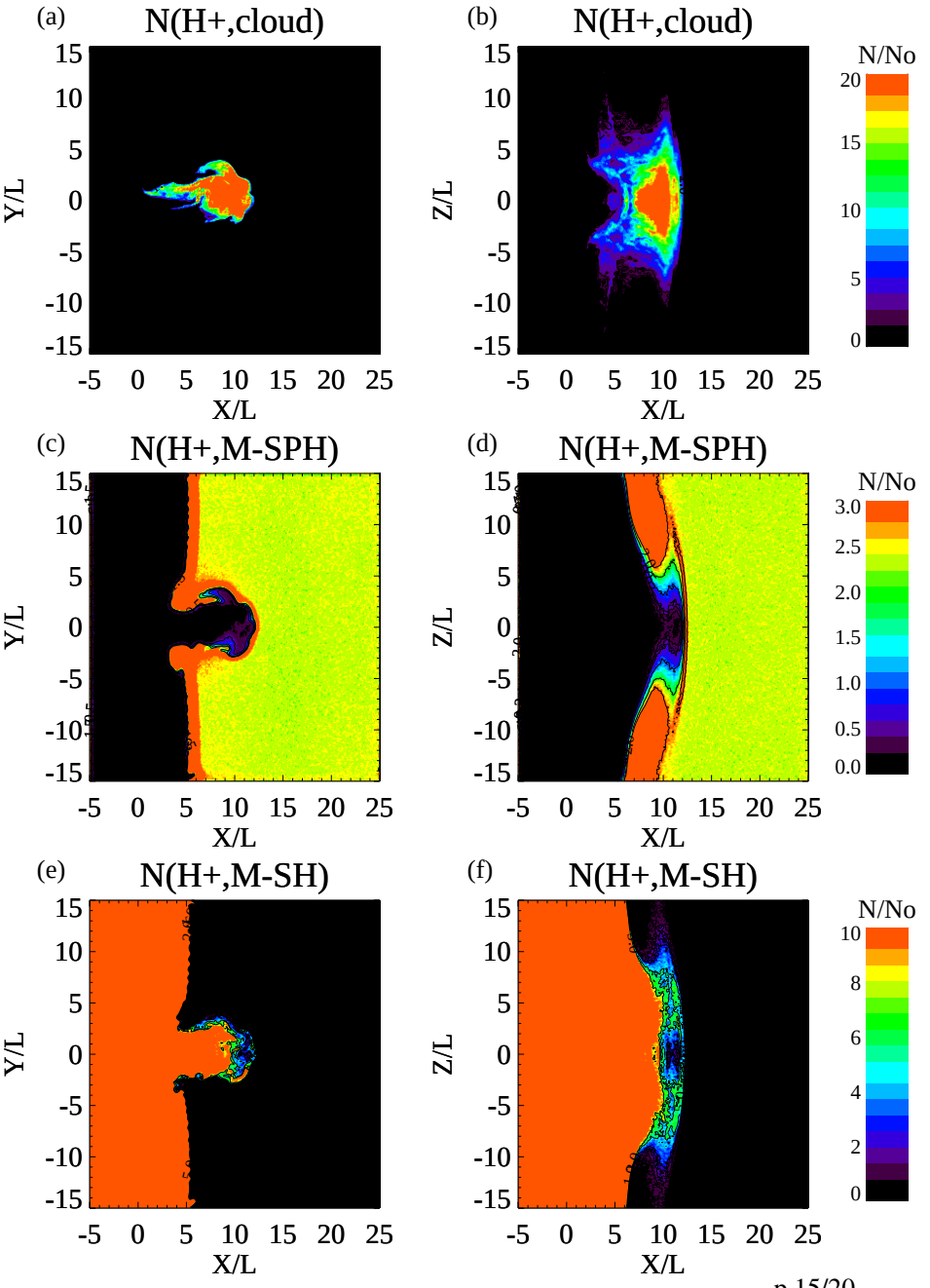

10. Plasma cloud penetration via magnetopause in case of low magnetosheath density and moderate initial speed

RUN – 84ghjc; $L = 400$ km;
Cloud speed $Ux = 350$ km/s;
Initial plasma density and
ion thermal velocity:
(a) Plasma cloud: $N_{i,cloud} \approx 110\,\mathrm{cm}^{-3}$;
$V_{th,i} \approx 20$ km/s;
(b) Magnetosheath: $N_i \approx 10\,\mathrm{cm}^{-3}$;
$V_{th,i} \approx 100$ km/s;
(c) Magnetosphere: $N_i \approx 2.4\,\mathrm{cm}^{-3}$;
$V_{th,i} \approx 100$ km/s.
Top: Cloud density;
Middle: Magnetospheric density;
Bottom: Magnetosheath density.

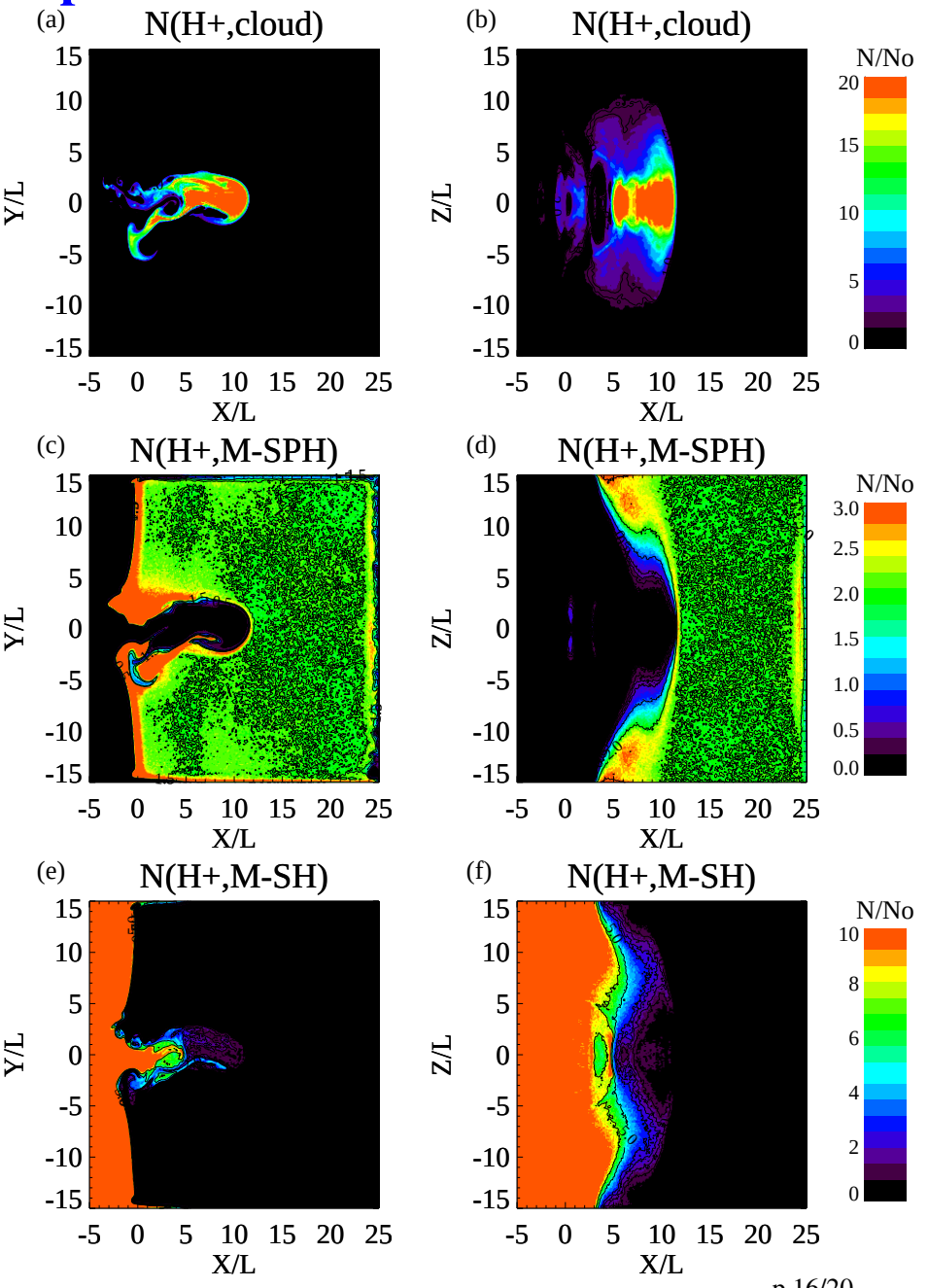

11. Exosphere of the Moon dynamics inside the Harris plasma sheet. From Lipatov,

Sarantos, Halekas, Cooper, Giles, Gershman (2023, unpublished)

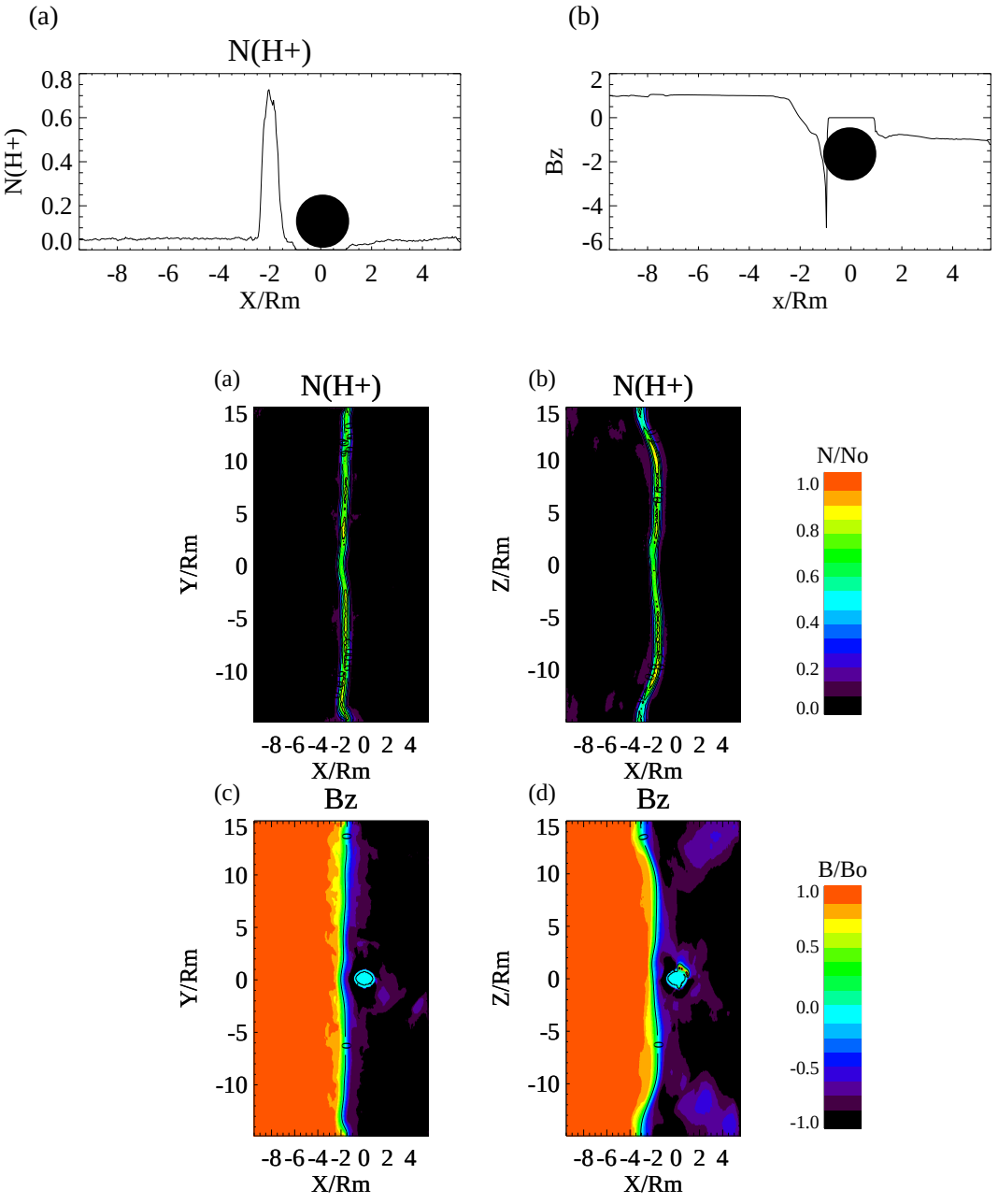

12. Effectivity of mass, momentum and energy transfer through TD

Case, L(km) Run	$U_{0,cloud}$(km/s) N_{msh}(cm^{-3})	R_{ci}(km) $\Delta_{cloud-mp}$(km)	$V_{th,i,msh}/W_0$ $V_{th,i,cloud}/W_0$	N_{cloud} (cm^{-3}) B_{msh} (nT)	$\frac{N_{cloud}}{N_{msh}}$ Effectivity
1, $L = 400$ ghc	700 10	230 2000	1.0 0.1	≈ 110 30	11 100 %
2, $L = 200$ ghkhha	700 60	230 1000	0.6 0.1	110 30	1.8 100%
3, $L = 400$ ghjc	350 10	116 2000	1.0 0.2	110 10	11 100%
4, $L = 200$ ghkhh	300 60	100 1000	0.6 0.1	110 30	1.8 10%
5, $L = 200$ ghkhhb	300 60	100 600	0.6 0.1	110 30	1.8 50%
6, $L = 400$ ghkk	300 60	100 600	0.6 0.1	60 30	1 $\approx 0\%$

Here, $U_{0,c}$(km/s), N_c (cm^{-3}) are the initial speed, density of the cloud; N_{msh}(cm^{-3}) and B_{msh} (nT) are magnetosheath density and magnetic field; R_{ci}(km) is the ion gyroradius; Δ_{c-mp}(km) are the initial distance between cloud and magnetopause; $V_{th,i,msh}/W_0$ and $V_{th,i,c}/W_0$ are the ion thermal velocity inside magnetosheath and clouds; $W_0 = 100$ km/s is a characteristic velocity; L is a characteristic lenght.

13. Summary

We use high-time-resolution data (150ms for ion and 30ms for electrons) from the MMS spacecraft along with hybrid kinetic **modeling with improved numerical resolution** to provide, for the first time, insights into the physics of wave–particle interactions triggered by dense plasma cloud penetration through the magnetopause considered as the tangential discontinuity. Results are summarized as follows:

- The cloud dynamics is controlled mainly by **the initial speed of the clouds**, **the ratio of the cloud/magnetosheath plasma density**, and **the ratio of the magnetospheric and magnetosheath magnetic field**;
- The **initial distance between the plasma cloud and magnetopause is also critical parameter** which determines the amount of magnetosheath plasma will by transfer into magnetosphere;
- The **performed modeling is also important** for understanding the wave-particle interactions **under penetration** of the **solar wind filamentary plasma elements, moons, and comets** (see e.g. Shoemaker-Levy 9 comet interaction with Jupiter modeling by Lipatov & Sharma, [GRL 1994]) **through the planetary bow shock and magnetopause**.
- The performed modeling may be important for understanding the penetration of the plasma cloud via heliopause.

14. Followup Work

Followup work will investigate:

- **Plasma cloud penetration through the TD with antiparallel magnetic field. Effects of magnetic reconnection on plasma cloud dynamics;**
- **Plasma cloud penetration through the rotational discontinuity (RD);**
- **Effects of plasma cloud penetration on the global perturbation of the magnetopause.**
- **Effects of the anomalous resistivity inside the magnetopause.**

Supported by NASA MMS Mission and the NASA SSW-2018 Award 80NSSC20K0146.